Flexural-torsional buckling of thin-walled composite box beams

Thuc Phuong Vo* and Jaehong Lee†

Department of Architectural Engineering, Sejong University
98 Kunja Dong, Kwangjin Ku, Seoul 143-747, Korea

(Dated: November 30, 2011)

Buckling of an axially loaded thin-walled laminated composite is studied. A general analytical model applicable to the flexural, torsional and flexural-torsional buckling of a thin-walled composite box beam subjected to axial load is developed. This model is based on the classical lamination theory, and accounts for the coupling of flexural and torsional modes for arbitrary laminate stacking sequence configuration, i.e. unsymmetric as well as symmetric, and various boundary conditions. A displacement-based one-dimensional finite element model is developed to predict critical loads and corresponding buckling modes for a thin-walled composite bar. Governing buckling equations are derived from the principle of the stationary value of total potential energy. Numerical results are obtained for axially loaded thin-walled composites addressing the effects of fiber angle, anisotropy, and boundary conditions on the critical buckling loads and mode shapes of the composites.

Keywords: Thin-walled composite, classical lamination theory, flexural-torsional vibration

I. INTRODUCTION

Fiber-reinforced composite materials have been used over the past few decades in a variety of structures. Composites have many desirable characteristics, such as high ratio of stiffness and strength to weight, corrosion resistance and magnetic transparency. Thin-walled structural shapes made up of composite materials, which are usually produced by pultrusion, are being increasingly used in many engineering fields. In particular, the use of pultruded composites in civil engineering structures await increased attention.

The theory of thin-walled closed section members made of isotropic materials was first developed by Vlasov [1] and Gjelsvik [2]. Many researchers have shown that thin-walled bars are susceptible to instability in a variety of modes, but a few publications have dealt with buckling behavior of such members. Closed-form solution for flexural and torsional buckling of isotropic thin-walled bars are found in the literature [3-4]. For composite thin-walled bars, the flexural and torsional buckling are fully coupled in general even for a doubly symmetric cross-section due to their material anisotropy. Bhaskar and Librescu [5] focused on the flexural buckling of single-cell extension-twist coupled beams under axial compression. The effects of direct transverse shear and the parasitic bending-transverse shear coupling as well as those of different boundary conditions and ply-angles were discussed. Shield and Morey [6] developed a new theory for analysis buckling of composite beams of open and closed cross section. The theory took into account deformation in the plane of the cross section due to anticlastic curvature. Suresh and Malhotra [7] studied buckling of laminated composite thin walled rectangular box beam configurations. The effect of number of layers, lay-up sequence and fiber angle on buckling load was analys for symmetric and anti-symmetric lay-ups. Recently, Cortinez and Piovan [8] presented the stability analysis of composite thin-walled beams with open or closed cross-sections. This model is based on the use of the Hellinger-Reissner principle, that considers shear flexibility in a full form, general cross-section shapes and symmetric balanced or especially orthotropic laminates. More recently, Piovan and Cortinez [9] developed a new theoretical model for the generalized linear analysis of composite thin-walled beams with open or closed cross-sections. This model allows studying many problems of static's, free vibrations with or without arbitrary initial stresses and linear stability of composite thin-walled beams with general cross-sections.

In the present study, the analytical model developed by Lee and Kim [10] and Vo and Lee [11] is extended to the buckling behavior of a thin-walled composite box beam. This model applicable to the flexural, torsional and flexural-torsional buckling of a thin-walled composite box beam subjected to axial load is developed. This model is

*Graduate student

†Associate Professor, corresponding author
; Electronic address: jhlee@sejong.ac.kr

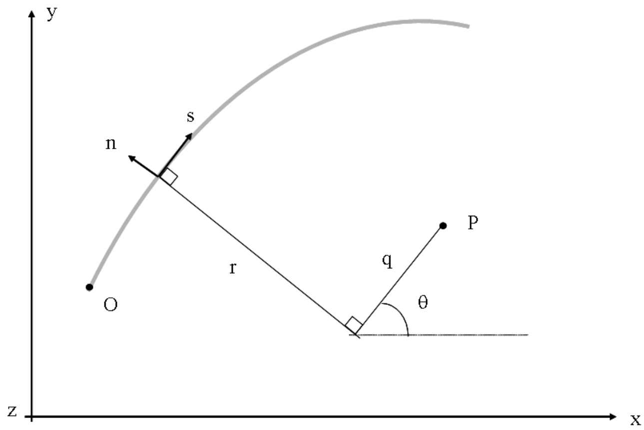

FIG. 1 Definition of coordinates in thin-walled closed sections

based on the classical lamination theory, and accounts for the coupling of flexural and torsional modes for arbitrary laminate stacking sequence configuration, i.e. unsymmetric as well as symmetric, and various boundary conditions. A displacement-based one-dimensional finite element model is developed to predict critical loads and corresponding buckling modes for a thin-walled composite bar. Governing buckling equations are derived from the principle of the stationary value of total potential energy. Numerical results are obtained for axially loaded thin-walled composites addressing the effects of fiber angle, anisotropy, and boundary conditions on the critical buckling loads and mode shapes of the composites.

II. KINEMATICS

The theoretical developments presented in this paper require two sets of coordinate systems which are mutually interrelated. The first coordinate system is the orthogonal Cartesian coordinate system (x, y, z), for which the x and y axes lie in the plane of the cross section and the z axis parallel to the longitudinal axis of the beam. The second coordinate system is the local plate coordinate (n, s, z) as shown in Fig.1, wherein the n axis is normal to the middle surface of a plate element, the s axis is tangent to the middle surface and is directed along the contour line of the cross section. The (n, s, z) and (x, y, z) coordinate systems are related through an angle of orientation θ as defined in Fig.1. Point P is called the pole axis, through which the axis parallel to the z axis is called the pole axis.

To derive the analytical model for a thin-walled composite beam, the following assumptions are made:

1. The contour of the thin wall does not deform in its own plane.
2. The linear shear strain $\bar{\gamma}_{sz}$ of the middle surface is to have the same distribution in the contour direction as it does in the St. Venant torsion in each element.
3. The Kirchhoff-Love assumption in classical plate theory remains valid for laminated composite thin-walled beams.
4. Each laminate is thin and perfectly bonded.
5. Local buckling is not considered.

According to assumption 1, the midsurface displacement components $\bar{u}, \bar{v}$ at a point A in the contour coordinate system can be expressed in terms of a displacements U, V of the pole P in the x, y directions, respectively, and the rotation angle Φ about the pole axis,

$$\bar{u}(s,z) = U(z)\sin\theta(s) - V(z)\cos\theta(s) - \Phi(z)q(s) \tag{1a}$$
$$\bar{v}(s,z) = U(z)\cos\theta(s) + V(z)\sin\theta(s) + \Phi(z)r(s) \tag{1b}$$

These equations apply to the whole contour. The out-of-plane shell displacement $\bar{w}$ can now be found from the assumption 2. For each element of middle surface, the shear strain become

$$\bar{\gamma}_{sz} = \frac{\partial \bar{v}}{\partial z} + \frac{\partial \bar{w}}{\partial s} = \Phi'(z)\frac{F(s)}{t(s)} \tag{2}$$

where $t(s)$ is thickness of contour box section, $F(s)$ is the St. Venant circuit shear flow.

After substituting for $\bar{v}$ from Eq.(1) and considering the following geometric relations,

$$\begin{aligned} dx &= ds\cos\theta && \text{(3a)}\\ dy &= ds\sin\theta && \text{(3b)}\end{aligned}$$

Eq.(2) can be integrated with respect to s from the origin to an arbitrary point on the contour,

$$\bar{w}(s,z) = W(z) - U'(z)x(s) - V'(z)y(s) - \Phi'(z)\omega(s) \tag{4}$$

where differentiation with respect to the axial coordinate z is denoted by primes ($'$); W represents the average axial displacement of the beam in the z direction; x and y are the coordinates of the contour in the (x, y, z) coordinate system; and ω is the so-called sectorial coordinate or warping function given by

$$\begin{aligned} \omega(s) &= \int_{s_\circ}^{s}\Big[r(s) - \frac{F(s)}{t(s)}\Big]ds && \text{(5a)}\\ \oint_i \frac{F(s)}{t(s)}ds &= 2A_i \quad i = 1, ..., n && \text{(5b)}\end{aligned}$$

where $r(s)$ is height of a triangle with the base ds; A_i is the area circumscribed by the contour of the i circuit. The explicit forms of $\omega(s)$ and $F(s)$ for box section are given in Ref.[11].

The displacement components u, v, w representing the deformation of any generic point on the profile section are given with respect to the midsurface displacements $\bar{u}, \bar{v}, \bar{w}$ by the assumption 3.

$$\begin{aligned} u(s,z,n) &= \bar{u}(s,z) && \text{(6a)}\\ v(s,z,n) &= \bar{v}(s,z) - n\frac{\partial\bar{u}(s,z)}{\partial s} && \text{(6b)}\\ w(s,z,n) &= \bar{w}(s,z) - n\frac{\partial\bar{u}(s,z)}{\partial z} && \text{(6c)}\end{aligned}$$

The strains associated with the small-displacement theory of elasticity are given by

$$\begin{aligned} \epsilon_s &= \bar{\epsilon}_s + n\bar{\kappa}_s && \text{(7a)}\\ \epsilon_z &= \bar{\epsilon}_z + n\bar{\kappa}_z && \text{(7b)}\\ \gamma_{sz} &= \bar{\gamma}_{sz} + n\bar{\kappa}_{sz} && \text{(7c)}\end{aligned}$$

where

$$\begin{aligned} \bar{\epsilon}_s &= \frac{\partial\bar{v}}{\partial s}; \quad \bar{\epsilon}_z = \frac{\partial\bar{w}}{\partial z} && \text{(8a)}\\ \bar{\kappa}_s &= -\frac{\partial^2\bar{u}}{\partial z^2}; \quad \bar{\kappa}_z = -\frac{\partial^2\bar{u}}{\partial z^2}; \quad \bar{\kappa}_{sz} = -2\frac{\partial^2\bar{u}}{\partial s\partial z} && \text{(8b)}\end{aligned}$$

All the other strains are identically zero. In Eq.(8), $\bar{\epsilon}_s$ and $\bar{\kappa}_s$ are assumed to be zero. $\bar{\epsilon}_z$, $\bar{\kappa}_z$ and $\bar{\kappa}_{sz}$ are midsurface axial strain and biaxial curvature of the shell, respectively. The above shell strains can be converted to beam strain components by substituting Eqs.(1), (4) and (6) into Eq.(8) as

$$\begin{aligned} \bar{\epsilon}_z &= \epsilon_z^\circ + x\kappa_y + y\kappa_x + \omega\kappa_\omega && \text{(9a)}\\ \bar{\kappa}_z &= \kappa_y\sin\theta - \kappa_x\cos\theta - \kappa_\omega q && \text{(9b)}\\ \bar{\kappa}_{sz} &= 2\bar{\chi}_{sz} = \kappa_{sz} && \text{(9c)}\end{aligned}$$

where $\epsilon_z^\circ, \kappa_x, \kappa_y, \kappa_\omega$ and κ_{sz} are axial strain, biaxial curvatures in the x and y direction, warping curvature with respect to the shear center, and twisting curvature in the beam, respectively defined as

$$\begin{aligned} \epsilon_z^\circ &= W' && \text{(10a)}\\ \kappa_x &= -V'' && \text{(10b)}\\ \kappa_y &= -U'' && \text{(10c)}\\ \kappa_\omega &= -\Phi'' && \text{(10d)}\\ \kappa_{sz} &= 2\Phi' && \text{(10e)}\end{aligned}$$

The resulting strains can be obtained from Eqs.(7) and (9) as

$$\begin{aligned}\epsilon_z &= \epsilon_z^\circ + (x + n\sin\theta)\kappa_y + (y - n\cos\theta)\kappa_x + (\omega - nq)\kappa_\omega &\text{(11a)}\\ \gamma_{sz} &= (n + \frac{F}{2t})\kappa_{sz} &\text{(11b)}\end{aligned}$$

III. VARIATIONAL FORMULATION

The total potential energy of the system can be stated, in its buckled shape, as

$$\Pi = \mathcal{U} + \mathcal{V} \tag{12}$$

where $\mathcal{U}$ is the strain energy

$$\mathcal{U} = \frac{1}{2}\int_v (\sigma_z\epsilon_z + \sigma_{sz}\gamma_{sz})dv \tag{13}$$

After substituting Eq.(11) into Eq.(13)

$$\mathcal{U} = \frac{1}{2}\int_v \Big\{\sigma_z\Big[\epsilon_z^\circ + (x + n\sin\theta)\kappa_y + (y - n\cos\theta)\kappa_x + (\omega - nq)\kappa_\omega\Big] + \sigma_{sz}(n + \frac{F}{2t})\kappa_{sz}\Big\}dv \tag{14}$$

The variation of strain energy can be stated as

$$\delta\mathcal{U} = \int_0^l (N_z\delta\epsilon_z + M_y\delta\kappa_y + M_x\delta\kappa_x + M_\omega\delta\kappa_\omega + M_t\delta\kappa_{sz})ds \tag{15}$$

where $N_z, M_x, M_y, M_\omega, M_t$ are axial force, bending moments in the x and y directions, warping moment (bimoment), and torsional moment with respect to the centroid, respectively, defined by integrating over the cross-sectional area as

$$\begin{aligned}N_z &= \int_A \sigma_z dsdn &\text{(16a)}\\ M_y &= \int_A \sigma_z(x + n\sin\theta)dsdn &\text{(16b)}\\ M_x &= \int_A \sigma_z(y - n\cos\theta)dsdn &\text{(16c)}\\ M_\omega &= \int_A \sigma_z(\omega - nq)dsdn &\text{(16d)}\\ M_t &= \int_A \sigma_{sz}(n + \frac{F}{2t})dsdn &\text{(16e)}\end{aligned}$$

The potential of in-plane loads $\mathcal{V}$ due to transverse deflection

$$\mathcal{V} = \frac{1}{2}\int_v \overline{\sigma}_z^0\Big[(u')^2 + (v')^2\Big]dv \tag{17}$$

where $\overline{\sigma}_z^0$ is the averaged constant in-plane edge axial stress, defined by $\overline{\sigma}_z^0 = P^0/A$. The variation of the potential of in-plane loads at the centroid is expressed by substituting the assumed displacement field into Eq.(17) as

$$\begin{aligned}\delta\mathcal{V} = &\int_v \frac{P^0}{A}\Big[U'\delta U' + V'\delta V' + (q^2 + r^2 + 2rn + n^2)\Phi'\delta\Phi' + (\Phi'\delta U' + U'\delta\Phi')\big[n\cos\theta - (y - y_p)\big]\\ &+ (\Phi'\delta V' + V'\delta\Phi')\big[n\cos\theta + (x - x_p)\big]\Big]dv \end{aligned}\tag{18}$$

In Eq. (18), the following geometric relations are used (Fig.1)

$$\begin{aligned}x - x_p &= q\cos\theta + r\sin\theta &\text{(19a)}\\ y - y_p &= q\sin\theta - r\cos\theta &\text{(19b)}\end{aligned}$$

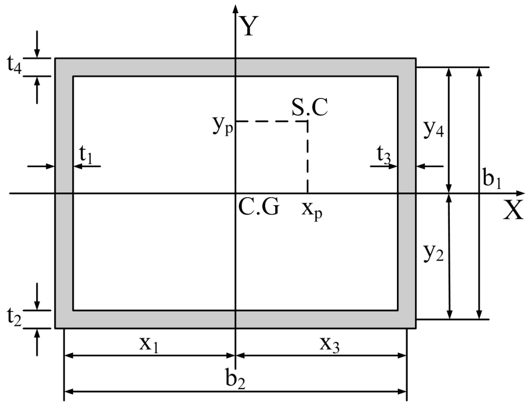

FIG. 2 Geometry of thin-walled composite box section

The principle of total potential energy can be stated as

$$\delta\Pi = \delta(\mathcal{U} + \mathcal{V}) = 0 \tag{20}$$

Substituting Eqs.(15) and (18) into Eq.(20), the following weak statement is obtained

$$\begin{aligned}\delta\Pi \; = \; & \int_0^l \Big[P^0 \big[\delta U'(U' + \Phi' y_p) + \delta V'(V' - \Phi' x_p) + \delta\Phi'(\Phi' \frac{I_p}{A} + U' y_p - V' x_p) \big] \\ + \; & N_z \delta W' + M_y \delta U'' + M_x \delta V'' + M_\omega \delta\Phi'' - 2M_t \delta\Phi \Big] dz \end{aligned} \tag{21}$$

IV. CONSTITUTIVE EQUATIONS

The constitutive equations of a k^{th} orthotropic lamina in the laminate co-ordinate system of box section are given by

$$\left\{ \begin{array}{c} \sigma_z \\ \sigma_{sz} \end{array} \right\}^k = \left[\begin{array}{cc} \bar{Q}^*_{11} & \bar{Q}^*_{16} \\ \bar{Q}^*_{16} & \bar{Q}^*_{66} \end{array} \right]^k \left\{ \begin{array}{c} \epsilon_z \\ \gamma_{sz} \end{array} \right\} \tag{22}$$

where $\bar{Q}^*_{ij}$ are transformed reduced stiffnesses. The transformed reduced stiffnesses can be calculated from the transformed stiffnesses based on the plane stress assumption and plane strain assumption. More detailed explanation can be found in Ref.[12]

The constitutive equations for bar forces and bar strains are obtained by using Eqs.(11), (16) and (22)

$$\left\{ \begin{array}{c} N_z \\ M_y \\ M_x \\ M_\omega \\ M_t \end{array} \right\} = \left[\begin{array}{ccccc} E_{11} & E_{12} & E_{13} & E_{14} & E_{15} \\ & E_{22} & E_{23} & E_{24} & E_{25} \\ & & E_{33} & E_{34} & E_{35} \\ & & & E_{44} & E_{45} \\ \text{sym.} & & & & E_{55} \end{array} \right] \left\{ \begin{array}{c} \epsilon^\circ_z \\ \kappa_y \\ \kappa_x \\ \kappa_\omega \\ \kappa_{sz} \end{array} \right\} \tag{23}$$

where E_{ij} are stiffnesses of the thin-walled composite, and can be defined by

$$E_{11} = \int_s A_{11} ds \tag{24a}$$

$$E_{12} = \int_s (A_{11} x + B_{11} \sin\theta) ds \tag{24b}$$

$$E_{13} = \int_s (A_{11} y - B_{11} \cos\theta) ds \tag{24c}$$

$$E_{14} = \int_s (A_{11}\omega - B_{11}q)ds \tag{24d}$$

$$E_{15} = \int_s (A_{16}\frac{F}{2t} + B_{16})ds \tag{24e}$$

$$E_{22} = \int_s (A_{11}x^2 + 2B_{11}x\sin\theta + D_{11}\sin^2\theta)ds \tag{24f}$$

$$E_{23} = \int_s \Big[A_{11}xy + B_{11}(y\sin\theta - x\cos\theta) - D_{11}\sin\theta\cos\theta\Big]ds \tag{24g}$$

$$E_{24} = \int_s \Big[A_{11}x\omega + B_{11}(\omega\sin\theta - qx) - D_{11}q\sin\theta\Big]ds \tag{24h}$$

$$E_{25} = \int_s \Big[A_{16}\frac{F}{2t}x + B_{16}(x + \frac{F\sin\theta}{2t}) + D_{16}\sin\theta\Big]ds \tag{24i}$$

$$E_{33} = \int_s (A_{11}y^2 - 2B_{11}y\cos\theta + D_{11}\cos^2\theta)ds \tag{24j}$$

$$E_{34} = \int_s \Big[A_{11}y\omega - B_{11}(\omega\cos\theta + qy) + D_{11}q\cos\theta\Big]ds \tag{24k}$$

$$E_{35} = \int_s \Big[A_{16}\frac{F}{2t}y + B_{16}(y - \frac{F\cos\theta}{2t}) - D_{16}\cos\theta\Big]ds \tag{24l}$$

$$E_{44} = \int_s (A_{11}\omega^2 - 2B_{11}\omega q + D_{11}q^2)ds \tag{24m}$$

$$E_{45} = \int_s \Big[A_{16}\frac{F}{2t}\omega + B_{16}(\omega - \frac{Fq}{2t}) - D_{16}q\Big]ds \tag{24n}$$

$$E_{55} = \int_s (A_{66}\frac{F^2}{4t^2} + B_{66}\frac{F}{t} + D_{66})ds \tag{24o}$$

where A_{ij}, B_{ij} and D_{ij} matrices are extensional, coupling and bending stiffness, respectively, defined by

$$(A_{ij}, B_{ij}, D_{ij}) = \int_n \bar{Q}_{ij}(1, n, n^2)dn \tag{25}$$

It appears that the laminate stiffnesses E_{ij} depend on the cross section of the composites. The explicit forms of them can be calculated for composite box section and given in Ref.[11].

V. GOVERNING EQUATIONS FOR BUCKLING

The buckling equations of the present study can be derived by integrating the derivatives of the varied quantities by parts and collecting the coefficients of of $\delta U, \delta V, \delta W$ and $\delta\Phi$

$$N_z' = 0 \tag{26a}$$

$$M_y'' + P^0(U'' + \Phi'' y_p) = 0 \tag{26b}$$

$$M_x'' + P^0(V'' - \Phi'' x_p) = 0 \tag{26c}$$

$$M_\omega'' + 2M_t' + P^0(\Phi''\frac{I_p}{A} + U''y_p - V''x_p) = 0 \tag{26d}$$

The natural boundary conditions are of the form

$$\delta W : N_z = N_z^0 \tag{27a}$$

$$\delta U : M_y' = M_y^{'0} \tag{27b}$$

$$\delta U' : M_y' = M_y^0 \tag{27c}$$

$$\delta V : M_x' = M_x^{'0} \tag{27d}$$

$$\delta V' : M_x' = M_x^0 \tag{27e}$$

$$\delta\Phi : M_\omega' + 2M_t = M_\omega^{'0} \tag{27f}$$

$$\delta\Phi' : M_\omega = M_\omega^0 \tag{27g}$$

where $N_z^0, M_y^{'0}, M_y^0, M_x^{'0}, M_x^0, M_\omega^{'0}, M_\omega^0$ are prescribed values. By substituting Eqs.(10) and (23) into Eq.(26) the explicit form of the governing equations can be expressed with respect to the laminate stiffnesses E_{ij} as

$$E_{11}W'' - E_{12}U''' - E_{13}V''' - E_{14}\Phi''' + 2E_{15}\Phi'' = 0 \tag{28a}$$
$$E_{12}W''' - E_{22}U^{iv} - E_{23}V^{iv} - E_{24}\Phi^{iv} + 2E_{25}\Phi''' + P^0(U'' + \Phi'' y_p) = 0 \tag{28b}$$
$$E_{13}W''' - E_{23}U^{iv} - E_{33}V^{iv} - E_{34}\Phi^{iv} + 2E_{35}\Phi''' + P^0(V'' - \Phi'' x_p) = 0 \tag{28c}$$
$$E_{14}W''' + 2E_{15}W'' - E_{24}U^{iv} - 2E_{25}U''' - E_{34}V^{iv} - 2E_{35}V''' - E_{44}\Phi^{iv} + 4E_{55}\Phi'' + P^0(\Phi''\frac{I_p}{A} + U''y_p - V''x_p) = 0 \tag{28d}$$

Eq.(28) is most general form for flexural-torsional buckling of a thin-walled laminated composite with a box section, and the dependent variables, U, V, W and Φ are fully coupled. If all the coupling effects are neglected and the cross section is symmetrical with respect to both x- and the y-axes, Eq.(28) can be simplified to the uncoupled differential equations as

$$(EA)_{com}W'' = 0 \tag{29a}$$
$$-(EI_y)_{com}U^{iv} + P^0U'' = 0 \tag{29b}$$
$$-(EI_x)_{com}V^{iv} + P^0V'' = 0 \tag{29c}$$
$$-(EI_\omega)_{com}\Phi^{iv} + \Big[(GJ)_{com} + P^0\frac{I_p}{A}\Big]\Phi'' = 0 \tag{29d}$$

From above equations, $(EA)_{com}$ represents axial rigidity, $(EI_x)_{com}$ and $(EI_y)_{com}$ represent flexural rigidities with respect to x and y axis, $(EI_\omega)_{com}$ represents warping rigidity, and $(GJ)_{com}$, represents torsional rigidity of the thin-walled composite, respectively, written as

$$(EA)_{com} = E_{11} \tag{30a}$$
$$(EI_y)_{com} = E_{22} \tag{30b}$$
$$(EI_x)_{com} = E_{33} \tag{30c}$$
$$(EI_\omega)_{com} = E_{44} \tag{30d}$$
$$(GJ)_{com} = 4E_{55} \tag{30e}$$

It is well known that the three distinct buckling modes, flexural buckling in the x and y direction, and torsional buckling, are identified in this case, and the corresponding buckling loads are given by the orthotropy solution for general boundary conditions [4]

$$P_x = \frac{\pi^2(EI_x)_{com}}{(K_xl)^2} \tag{31a}$$
$$P_y = \frac{\pi^2(EI_y)_{com}}{(K_yl)^2} \tag{31b}$$
$$P_0 = \frac{A}{I_p}\Big[\frac{\pi^2(EI_\omega)_{com}}{(K_0l)^2} + (GJ)_{com}\Big] \tag{31c}$$

where P_x, P_y, P_0 are flexural buckling loads in the x and y direction, and torsional buckling load. For simply-supported and cantilever beams, $K_x = K_y = K_0 = 1$ and $K_x = K_y = K_0 = 2$, respectively.

VI. FINITE ELEMENT FORMULATION

The present theory for thin-walled composite beams described in the previous section was implemented via a displacement based finite element method. The generalized displacements are expressed over each element as a linear combination of the one-dimensional Lagrange interpolation function Ψ_j and Hermite-cubic interpolation function ψ_j

associated with node j and the nodal values

$$W = \sum_{j=1}^{n} w_j \Psi_j \tag{32a}$$

$$U = \sum_{j=1}^{n} u_j \psi_j \tag{32b}$$

$$V = \sum_{j=1}^{n} v_j \psi_j \tag{32c}$$

$$\Phi = \sum_{j=1}^{n} \phi_j \psi_j \tag{32d}$$

Substituting these expressions into the weak statement in Eq.(18), the finite element model of a typical element can be expressed as the standard eigenvalue problem

$$([K] - \lambda[G])\{\Delta\} = \{0\} \tag{33}$$

where $[K]$ is the element stiffness matrix

$$[K] = \begin{bmatrix} K_{11} & K_{12} & K_{13} & K_{14} \\ & K_{22} & K_{23} & K_{24} \\ & & K_{33} & K_{34} \\ \text{sym.} & & & K_{44} \end{bmatrix} \tag{34}$$

and $[G]$ is the element geometric stiffness matrix

$$[G] = \begin{bmatrix} G_{11} & G_{12} & G_{13} & G_{14} \\ & G_{22} & G_{23} & G_{24} \\ & & G_{33} & G_{34} \\ \text{sym.} & & & G_{44} \end{bmatrix} \tag{35}$$

The explicit forms of $[K]$ and $[G]$ are given by

$$K_{ij}^{11} = \int_0^l E_{11} \Psi_i' \Psi_j' dz \tag{36a}$$

$$K_{ij}^{12} = -\int_0^l E_{12} \Psi_i' \psi_j'' dz \tag{36b}$$

$$K_{ij}^{13} = -\int_0^l E_{13} \Psi_i' \psi_j'' dz \tag{36c}$$

$$K_{ij}^{14} = \int_0^l (2E_{15} \Psi_i' \psi_j' - E_{14} \Psi_i' \psi_j'') dz \tag{36d}$$

$$K_{ij}^{22} = \int_0^l E_{22} \psi_i'' \psi_j'' dz \tag{36e}$$

$$K_{ij}^{23} = \int_0^l E_{23} \psi_i'' \psi_j'' dz \tag{36f}$$

$$K_{ij}^{24} = \int_0^l (E_{24} \psi_i'' \psi_j'' - 2E_{25} \psi_i'' \psi_j') dz \tag{36g}$$

$$K_{ij}^{33} = \int_0^l E_{33} \psi_i'' \psi_j'' dz \tag{36h}$$

$$K_{ij}^{34} = \int_0^l (E_{34} \psi_i'' \psi_j'' - 2E_{35} \psi_i'' \psi_j') dz \tag{36i}$$

TABLE I Buckling loads with different stacking sequences and boundary conditions

Boundary conditions	Stacking sequence	Ref.[8]	Present
Simly Supported-	[0/0/0/0]	5.235	5.196
Simly Supported	[0/90/90/0]	2.810	2.777
	[45/-45/-45/45]	0.546	0.541
Clamp-Clamp	[0/0/0/0]	20.867	20.785
	[0/90/90/0]	11.270	11.111
	[45/-45/-45/45]	2.175	2.166
Clamp-	[0/0/0/0]	10.696	10.630
Simly Supported	[0/90/90/0]	5.776	5.682
	[45/-45/-45/45]	1.115	1.108
Clamp-Free	[0/0/0/0]	1.310	1.299
	[0/90/90/0]	0.707	0.694
	[45/-45/-45/45]	0.137	0.135

$$K_{ij}^{44} = \int_0^l (E_{44}\psi_i''\psi_j'' - 2E_{45}(\psi_i'\psi_j'' + \psi_i''\psi_j') + 4E_{55}\psi_i'\psi_j')dz \tag{36j}$$

$$G_{ij}^{22} = G_{ij}^{33} = \int_0^l \psi_i'\psi_j' dz \tag{36k}$$

$$G_{ij}^{24} = \int_0^l y_p\psi_i'\psi_j' dz \tag{36l}$$

$$G_{ij}^{34} = -\int_0^l x_p\psi_i'\psi_j' dz \tag{36m}$$

$$G_{ij}^{44} = \int_0^l \frac{I_p}{A}\psi_i'\psi_j' dz \tag{36n}$$

All other components are zero. In Eq.(33), $\{\Delta\}$ is the eigenvector of nodal displacements corresponding to an eigenvalue

$$\{\Delta\} = \{W\ U\ V\ \Phi\}^{\mathrm{T}} \tag{37}$$

VII. NUMERICAL EXAMPLES

For verification purpose, a composite box beam with length $l = 4$m and the cross section as shown in Fig.3a with different stacking sequences and boundary conditions under axial load is considered. Plane stress assumption ($\sigma_s = 0$) is made in the analysis. The following material properties are used (Ref.[8])

$$E_1 = 144\text{GPa}\ , E_2 = 9.65\text{GPa}\ , G_{12} = 4.14\text{GPa}\ , \nu_{12} = 0.3 \tag{38}$$

The results using the present analysis are compared with previously available results in Table I. It is seen that the results by the present finite element analysis are in good agreement with the solution in Ref.[8].

In order to investigate the effects of fiber orientation, and boundary conditions on the buckling loads and the mode shapes, a thin-walled composite box beam with the same cross section and the length $l = 8$m under axial load is considered. The results are reported for composite beam with simply supported and cantilever boundary conditions. The following engineering constants are used

$$E_1/E_2 = 25, G_{12}/E_2 = 0.6, \nu_{12} = 0.25 \tag{39}$$

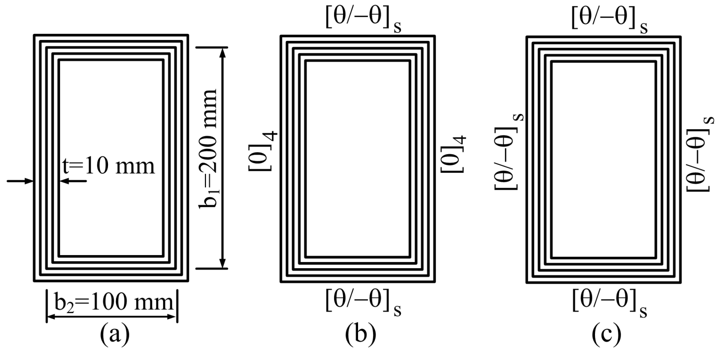

FIG. 3 Thin-walled composite box beam and two stacking sequences

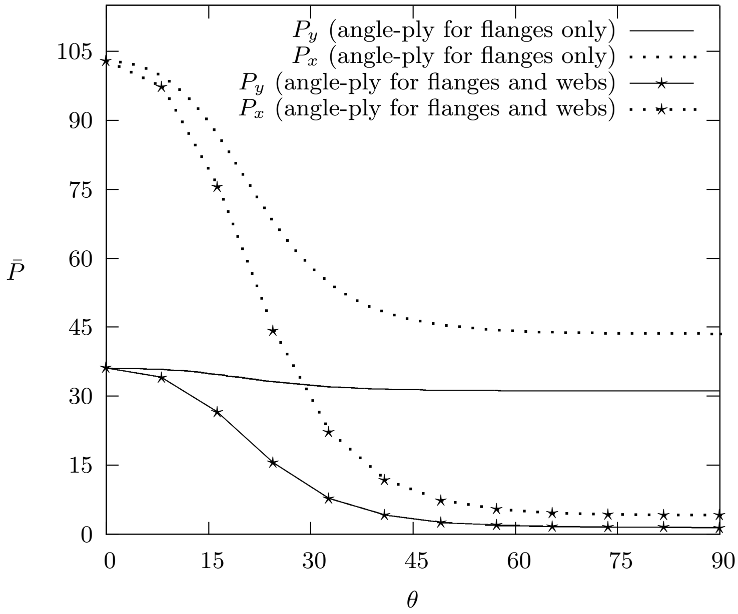

FIG. 4 Variation of the critical flexural buckling loads of the weak and strong axis with respect to fiber angle change in the webs and flanges for a simply supported composite beam

For convenience, the following nondimensional buckling load is used

$$\bar{P} = \frac{Pl^2}{b_1^3 t E_2} \tag{40}$$

A simply supported composite beam with two different stacking sequences is considered. Firstly, symmetric angle-ply laminate $[\theta/-\theta]_s$ in the flanges, while the webs are assumed unidirectional, (Fig.3b). Secondly, both the flanges and webs are assumed to be symmetric angle-ply stacking sequence, (Fig.3c). For two cases considered, the flange and the web laminates are balanced symmetric and thus, all the coupling stiffnesses become zero. Accordingly, the flexural buckling and the torsional buckling are uncoupled, and the solution can be given in the orthotropy solution as in Eqs.(31a)-(31c). The buckling loads of the three distinct modes, the flexural mode in the x- and y-direction and the torsional mode, by the finite element analysis are compared to those of the orthotropy solution with fiber angle change in the flanges and webs. Excellent agreements are made between two results as given in Figs.4 and 5. This is because of the fact that all the coupling stiffnesses vanish in these cases, and thus, the orthotropy solution given in Eqs.(31a)-(31c) is sufficiently accurate in predicting buckling loads. It is seen that the buckling load for the torsional mode is well above the other two types of buckling loads, i.e. P_x and P_y.

The next example is a cantilever composite beam with the left and right webs are considered as $[-\theta_2]$ and $[\theta_2]$ respectively, while the flanges are unidirectional. All coupling stiffnesses are zero, but E_{25} does not vanish due to

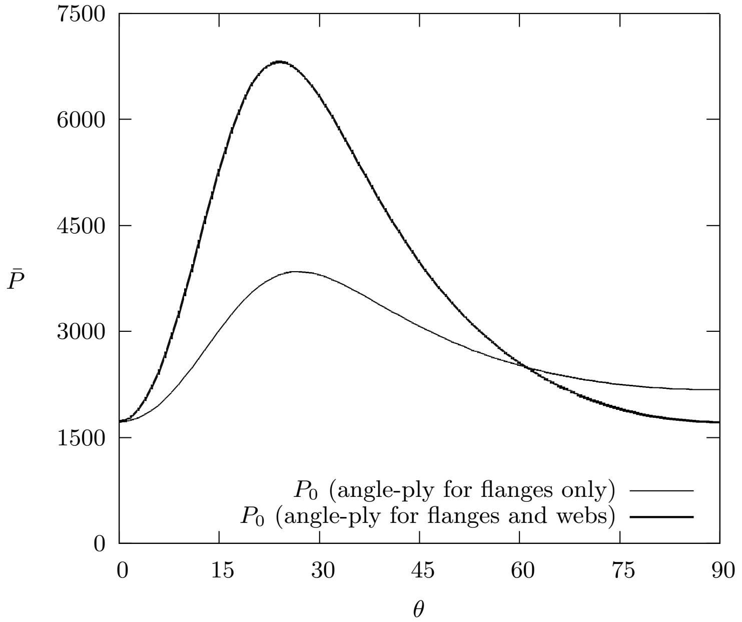

FIG. 5 Variation of the critical torsional buckling loads with respect to fiber angle change in the webs and flanges for a simply supported composite beam

unsymmetric stacking sequence of the webs. Accordingly, the flexural buckling in the x-direction is uncoupled, whereas the flexural buckling in the y-direction and the torsional buckling are coupled. The critical buckling loads by the finite element analysis and the orthotropy solution, which neglects the coupling effects of E_{25} , from Eqs.(31a)-(31c) are shown in Fig.6. For unidirectional fiber direction, the critical buckling loads by the finite element analysis exactly correspond to the flexural buckling loads in y-direction. The mode shape corresponding to the critical buckling load with fiber angle $\theta = 15°$ is illustrated in Fig.7. It can be seen that the critical buckling mode shape exhibits double coupling (the flexural mode in y-direction and the torsional mode). Due to the large coupling stiffnesses E_{25} in the range of ($\theta = 5° - 45°$), this mode become predominantly flexural y-direction mode, with a little contribution from torsion. Therefore, the results by finite element analysis and orthotropy solution show discrepancy in this range. As the fiber angle increases, the coupling stiffnesses E_{25} become small. Therefore, the critical buckling mode is purely flexural y-direction mode as shown in Fig.8 and thus, the results by othotropy solution and finite element analysis are identical.

In order to investigate the coupling effect further, the top flange and the left web are considered as $[0°/-\theta_2/90°]$ and $[0°/\theta_2/90°]$, while the bottom flange and the right web are $[45^\circ_4]$. For this stacking sequence, the coupling stiffnesses $E_{12}, E_{13}, E_{15}, E_{25}$ and E_{35} become no more negligibly small. The mode shape corresponding to the critical buckling load with with fiber angle $\theta = 15°$ is illustrated in Fig.10. Relative measures of the flexural displacements and the torsional rotation show that the mode is triply coupled mode (the flexural mode in the x- and y-directions and the torsional mode). This fact explains as the fiber angle changes, the orthotropy solution and finite element analysis solution show remarkably discrepancy indicating the coupling effects become significant. As fiber angle increases, since the coupling stiffnesses decrease, the discrepancy becomes small. That is, the orthotropy solution is no longer valid for unsymmetrically laminated beams, and triply coupled flexural-torsional buckling should be considered even for a double symmetric cross-section.

VIII. CONCLUDING REMARKS

An analytical model was developed to study the flexural-torsional buckling of a laminated composite box beam under axial load. The model is capable of predicting accurate buckling load as well as buckling mode shapes for various configuration including boundary conditions, laminate orientation of the composite beams. To formulate the problem, a one-dimensional displacement-based finite element method is employed. All of the possible buckling modes including the flexural mode in the x and y-direction and the torsional mode, and fully coupled flexural-torsional mode are included in the analysis. The model presented is found to be appropriate and efficient in analyzing buckling problem of a thin-walled laminated composite beam under axial load.

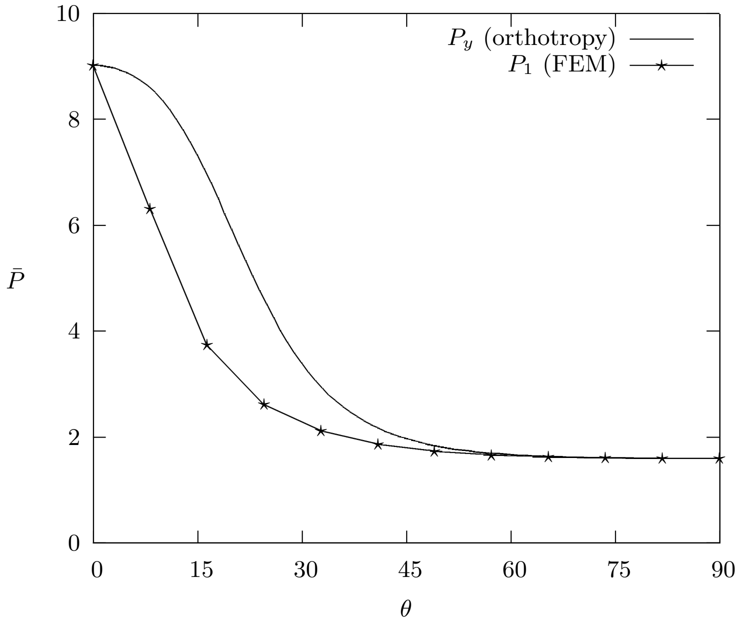

FIG. 6 Variation of the critical buckling loads with respect to fiber angle change in the webs for a cantilever composite beam

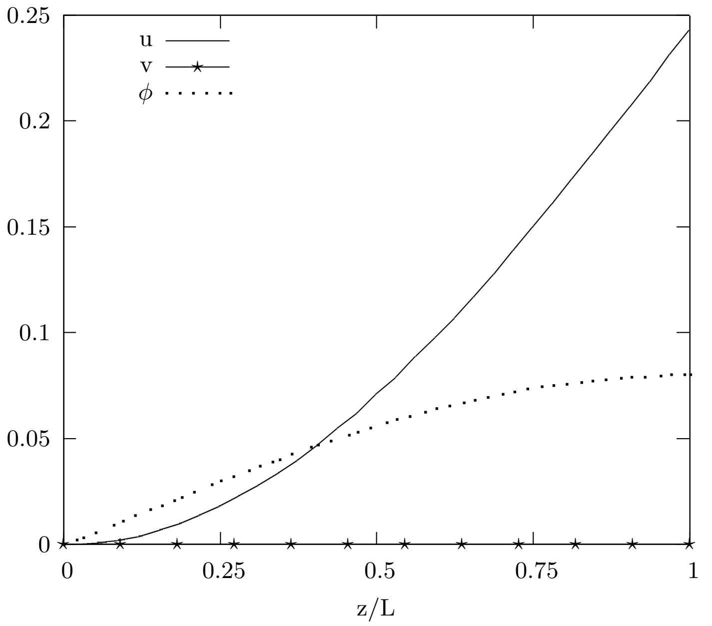

FIG. 7 Mode shapes of the flexural and torsional components for $P_1 = 4.042$ of a cantilever composite beams with the fiber angle 15° in the top flange and the left web

Acknowledgments

The support of the research reported here by Korea Ministry of Construction and Transportation through Grant 2006-C106A1030001-06A050300220 is gratefully acknowledged.

References

[1] Vlasov, V. Z., *Thin-walled elastic beams*, 2nd Edition, Israel Program for Scientific Translation, Jerusalem, Israel, 1961.

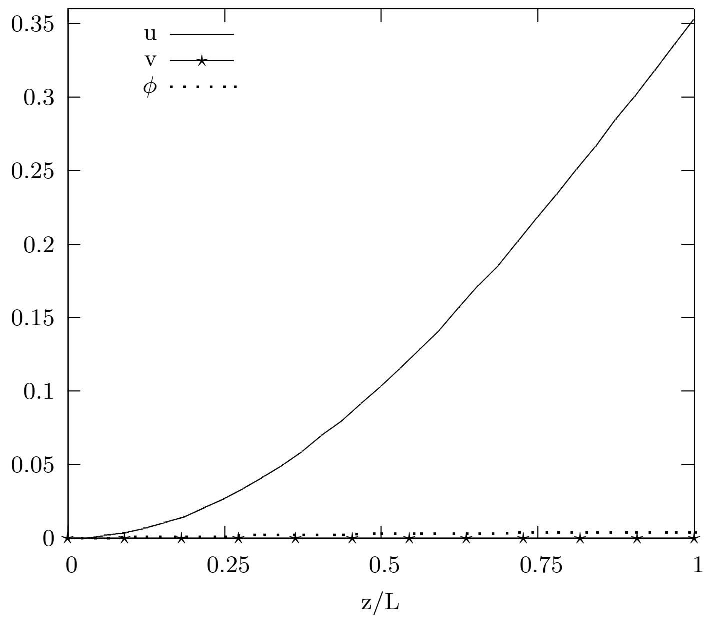

FIG. 8 Mode shapes of the flexural and torsional components for $P_1 = 1.603$ of a cantilever composite beams with the fiber angle 75° in the top flange and the left web

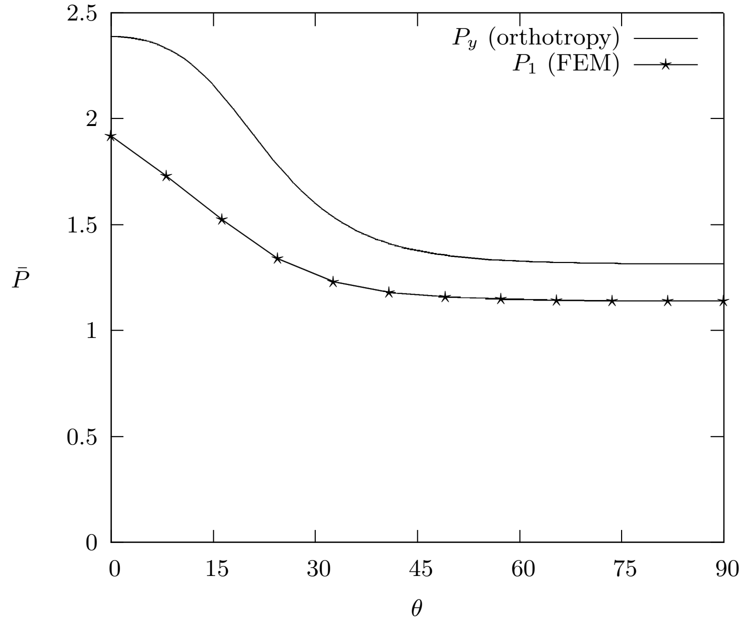

FIG. 9 Variation of the critical buckling load with respect to fiber angle change in the top flange and the left web for a cantilever composite beam

[2] Gjelsvik, A., *The theory of thin-walled bars*, John Wiley and Sons Inc., New York, 1981.
[3] Timoshenko, S. P. and Gere, J.M., *Theory of elastic stability*, McGraw-Hill, New York, 1963.
[4] Trahair, N.S., *Flexural-torsional buckling of structures*, CRC Press, London, 1993.
[5] Bhaskar, K., and Librescu, L., "Buckling under axial compression of thin-walled composite beams exhibiting extension-twist coupling," *Composite Structures*, Vol.31, 1995, pp.203-212.
[6] Shield, C.K and Morey T.A, "Kinematic theory of open and closed section thin-walled composite beams," *Journal of Engineering Mechanics*, Vol.123, No. 10, 1997, pp.1070-1081.
[7] Suresh, R. and Malhotra, S.K., "Some studies on buckling of laminated composite thin walled box beams," *Composite Structures*, Vol.40, No. 3-4, 1998, pp.267-275.

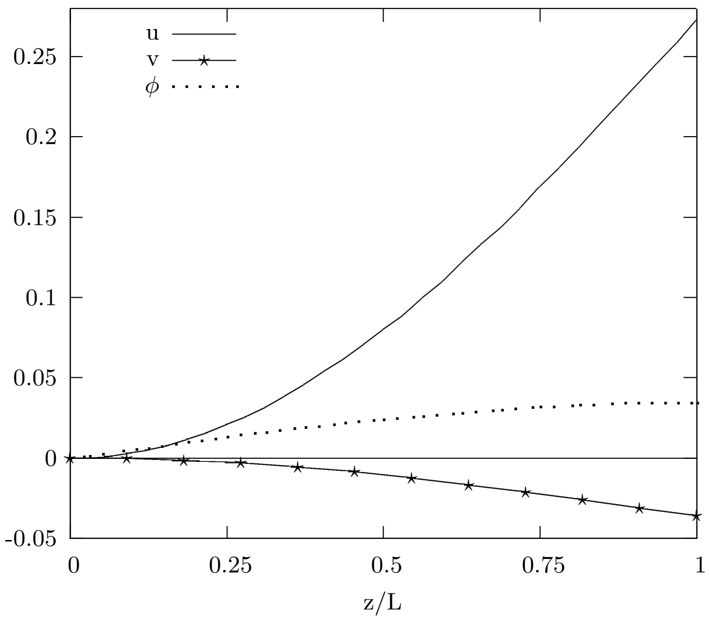

FIG. 10 Mode shapes of the flexural and torsional components for $P_1 = 1.557$ of a cantilever composite beam with the fiber angle 15° in the top flange and the left web

[8] Cortinez, V.H. and Piovan, M.T., "Stability of composite thin-walled beams with shear deformability," *Computers and Structures*, Vol.84, 2006, pp. 978-990.

[9] Piovan, M.T. and Cortinez, V.H., "Mechanics of shear deformable thin-walled beams made of composite materials," *Thin-Walled Structures*, Vol.45, 2007, pp. 37-62.

[10] Lee, J. and Kim, S., "Flexural-torsional buckling of thin-walled I-section composites," *Computers and Structures*, Vol.79, 2001, pp.987-995.

[11] Vo, T.P. and Lee, J., "Flexural-torsional behavior of thin-walled closed-section composite box beams," *Engineering Structures*, In Press, Vol.29, 2007

[12] Jones, R. M., *Mechanics of composite materials*, Hemisphere Publishing Corp., New York, 1975.